Efficient Prestimulus Network Integration of Fusiform Face Area Biases Face Perception during Binocular Rivalry

Elie Rassi[1,2], Andreas Wutz[1,3], Nicholas Peatfield[4], and Nathan Weisz[1,4,5]

Abstract

■ Ongoing fluctuations in neural excitability and connectivity influence whether or not a stimulus is seen. Do they also influence which stimulus is seen? We recorded magnetoencephalography data while 21 human participants viewed face or house stimuli, either one at a time or under bistable conditions induced through binocular rivalry. Multivariate pattern analysis revealed common neural substrates for rivalrous versus nonrivalrous stimuli with an additional delay of ~36 msec for the bistable stimulus, and poststimulus signals were source-localized to the fusiform face area. Before stimulus onset followed by a face versus house report, fusiform face area showed stronger connectivity to primary visual cortex and to the rest of the cortex in the alpha frequency range (8–13 Hz), but there were no differences in local oscillatory alpha power. The prestimulus connectivity metrics predicted the accuracy of poststimulus decoding and the delay associated with rivalry disambiguation suggesting that perceptual content is shaped by ongoing neural network states. ■

INTRODUCTION

Ongoing neural fluctuations interact with sensory inputs and influence perception (Sadaghiani, Hesselmann, & Kleinschmidt, 2009; Boly et al., 2007). These interactions can be captured by characterizing prestimulus brain activity and the influence of that activity on upcoming perception and behavior. For example, prestimulus oscillatory power, an index of neural excitability, influences whether or not a near-threshold stimulus will be detected (Benwell et al., 2017; Iemi, Chaumon, Crouzet, & Busch, 2017; Hanslmayr et al., 2007; Ergenoglu et al., 2004). Considering the complex spatio-temporal properties of ongoing neural activity, connectivity measures have also been used to better understand prestimulus brain states. As a result, prestimulus connectivity was also shown to influence near-threshold perception (Frey et al., 2016; Leonardelli et al., 2015; Leske et al., 2015; Weisz et al., 2014).

However, beyond mere stimulus detection, one of the most important functions of the visual system is categorizing objects, thereby building the contents of visual experiences (Wutz, Melcher, & Samaha, 2018; Miller, Nieder, Freedman, & Wallis, 2003; Logothetis & Sheinberg, 1996). To distill the neural correlates of visual content, researchers have employed bistable perception paradigms in which the perceived category of an ambiguous but invariant stimulus can switch over time (Leopold & Logothetis, 1996). Examples of bistable stimuli include the Necker cube (Necker, 1832), the Rubin vase (Rubin, 1915), and binocular rivalry (Walker, 1978). When bistable stimuli are presented briefly, only one of the two possible interpretations of the ambiguous image is perceived. Over multiple presentations, perception of the stimulus will vary between the two interpretations. This trial-by-trial variance in perception can then be used to assess the prestimulus patterns that might have influenced perception of one or the other stimulus category (Rassi, Fuscà, Weisz, & Demarchi, 2019; Rassi, Wutz, Müller-Voggel, & Weisz, 2019). As such, briefly presented bistable images are unique tools to probe the influence of prestimulus neural activity on subsequent perception. Given that prestimulus neural excitability and connectivity bias stimulus detection ("Did you see anything?"), here we ask whether they also bias perceptual content ("What did you see?").

Previous studies that have used bistable stimuli with semantic content, such as the faces and the vase of the Rubin vase, have reported the involvement of temporal cortical regions known to be involved in nonrivalrous object perception. For example, an fMRI study using the Rubin vase illusion reported increased prestimulus fusiform face area (FFA) activity before face (vs. vase) reports (Hesselmann, Kell, Eger, & Kleinschmidt, 2008), and our magnetoencephalography (MEG) study using the same stimulus reported increased prestimulus connectivity between the FFA and early visual cortex before face (vs. vase) reports (Rassi, Wutz, et al., 2019). The connectivity patterns in that MEG study were found in the frequency range between 5 and 20 Hz covering theta, alpha, and

[1]University of Salzburg, [2]Radboud University, Nijmegen, The Netherlands, [3]Massachusetts Institute of Technology, [4]University of Trento, Rovereto, Italy, [5]Paracelsus Medical University, Salzburg, Austria

Journal of Cognitive Neuroscience 34:6, pp. 1001–1014
https://doi.org/10.1162/jocn_a_01843

lower beta oscillations. Among those, the effects were most pronounced in the alpha frequency range (~8–13 Hz). Alpha oscillations are the most prominent rhythm in the human brain and have been functionally linked with neural excitation and inhibition (Jensen & Mazaheri, 2010; Klimesch, Sauseng, & Hanslmayr, 2007; Başar, Gönder, & Ungan, 1976).

Although the ambiguity of the Rubin vase illusion is likely resolved by means of figure–ground segregation (Pitts, Martínez, Brewer, & Hillyard, 2011; Hasson, Hendler, Bashat, & Malach, 2001; Rubin, 1915), the perceptual processes involved in resolving binocular rivalry are less clear and still a matter of debate (Panagiotaropoulos, Dwarakanath, & Kapoor, 2020; Brascamp, Sterzer, Blake, & Knapen, 2018). Even less known is the effect of ongoing prestimulus brain activity on resolving binocular rivalry, as the rivalrous stimulus is typically presented continuously to investigate the neural correlates of perceptual "switches," or alternations between the two percepts (Abdallah & Brooks, 2020; Tong, Nakayama, Vaughan, & Kanwisher, 1998). To probe possible prestimulus effects at rivalry onset, the rivalrous stimulus would have to be presented briefly in between periods of no presentation. Such a setup, in combination with the high temporal resolution of MEG, would further allow to explore the temporal dynamics of rivalry resolution or disambiguation, as compared to nonrivalrous perception.

On the basis of the "Windows to Consciousness" framework (Ruhnau, Hauswald, & Weisz, 2014; Weisz et al., 2014), fluctuating connectivity levels influence upcoming perception and neural signals associated with perception. In particular, it states that the network integration of brain regions, which are crucial for mediating a particular perceptual experience (so-called essential nodes; Zeki & Bartels, 1999), will bias further processing, because more strongly integrated regions are more likely to broadly distribute its activity. The extent of network integration can be quantified using measures from graph theory such as efficiency (Weisz et al., 2014; Bullmore & Sporns, 2009).

In this MEG study, we used a brief-presentation binocular rivalry setup with the classical face-and-house combination. Treating the FFA as an essential node, we investigated whether prestimulus neural excitability and/or network integration of this region influences the disambiguation and perceptual report of the rivalrous stimuli and whether the relevant prestimulus patterns also influence the corresponding poststimulus neural activity. We predicted increased connectivity between FFA and the rest of the brain and, more specifically, between FFA and V1, before "face" (vs. "house") reports. In addition, we aimed to test how the neural activity associated with perceiving the bistable stimulus related to that associated with perceiving unambiguous stimuli. For this purpose, we also employed a passive viewing task (oddball design) and predicted that processing the bistable and unambiguous stimuli share neural substrates but that the content of unambiguous stimuli can be decoded earlier in time compared to the bistable stimulus.

METHODS

Participants

Twenty-three volunteers with normal or corrected-to-normal vision participated in this experiment. We excluded two participants as their MEG data were excessively noisy, ending up with 21 participants (11 men and 10 women, three left-handed; mean age = 26.3 years, *SD* = 3.7 years, range = 22–35 years). Because this experiment was conceived as a conceptual follow-up to our previous work (Rassi, Wutz, et al., 2019; Weisz et al., 2014), we chose this number of participants such that the experiment is similarly powered. During the course of the experiment, participants wore nonmagnetic clothes, and a questionnaire before the experiment excluded any metal artifacts on the participants' body. The ethics committee of the University of Trento approved the experimental procedure, and all participants gave written informed consent before taking part in the study.

Experimental Procedure

Participants were seated upright in the MEG system, and we instructed them to keep fixation and to avoid eye blinks and movements as best as possible during the experiment. To create rivalry, we used blue/red filter glasses, which participants wore throughout. We took into account the color filters and, as such, adapted the stimulus to suit the glasses. In between the blocks, participants had a short break but remained seated in the MEG system. We displayed visual stimuli via a video projector outside the MEG chamber, which projected to a screen in the MEG chamber. A camera allowed us to monitor participants during the experiment. We measured the head position in between blocks, once at the beginning of each block for later offline use, after having instructed participants to readjust their head position to their perceived initial position.

Stimuli

The experiment was divided into three different task types: staircase thresholding, passive viewing/oddball task, and onset binocular rivalry. We programmed and controlled all experiments in Psychtoolbox (Kleiner et al., 2007) and the DataPixx I/O Controller and back-projected using the ProPixx Projector at 120 Hz at 1980 × 1080 with the central images 400 × 400 in size and presented at a distance of 78 cm. The size of the images was 14.8° of visual angle.

We generated the face image with the facegen software (facegen.com/), took the house image from the Pasadena

Houses database (www.vision.caltech.edu/html-files/archive.html), and masked their backgrounds in black. See the face and house images in Figure 1 for the actual images used in the main experiment.

In the passive viewing task, we used 160 unique, black-and-white images of faces and houses (80 each). In the staircase procedure and the main task, we used the same two images (one face and one house; not included in the pool presented during passive viewing). That is, there were two combinations of one face and one house image: red face/blue house and blue face/red house (each presented 240 times). So it was the same face (or house) regardless of whether it was red or blue. The colors of the face and house images (red or blue) were counterbalanced across trials, so each eye would receive an equal number of face and house (and an equal number of red and blue) images.

Staircase Procedure

Because of the competing face/house stimulus properties, we wanted to ensure that participants perceived roughly equal numbers of houses and faces. As such, we ran a staircase thresholding procedure with the MATLAB (The MathWorks, Inc.) toolbox Palamedes (Prins & Kingdom, 2018). Four staircase procedures controlled the brightness of the red house, blue house, red face, and blue face stimuli. The procedure was a simple 1-up 1-down with a step size of 0.01, a start value of 0.5, a minimum/maximum of 0.95/0.05, and a stop rule at 32 reversals (where a reversal is an up after a down or vice versa).

In arbitrary units where the total brightness of each stimulus was 1, the blue house/red face stimulus consisted on average of .57 blue house (and therefore .43 red face, SD = .32), whereas the blue face/red house stimulus consisted of .165 blue face (and therefore .835 red house, SD = .24). That is, in both cases, the brightness of red had to be decreased relative to the brightness of blue.

Passive Viewing/Oddball Task

To compare the neural responses to rivalrous and unambiguous stimuli, we presented participants with unambiguous house and face images (80 of each) before the main experiment. A stimulus would appear for 500 msec, followed by a jittered ISI of 1–2 sec, during which a fixation cross would appear. We required participants to report an oddball (inverted house or face) occurring on 10% of the trials to keep them engaged in the viewing task. During this task, participants did not wear the red/blue filter glasses.

Onset Binocular Rivalry (Main Task)

In the main experiment, we presented participants with the rivalrous face/house images and required them to report their percept on each trial. A trial would begin with the presentation of a central fixation cross, followed by a blank screen for jittered interval of 1–2 sec. After the blank screen, the bistable image would appear for 500 msec, and then a response screen "House or Face?" would appear, the prompt for participants to respond

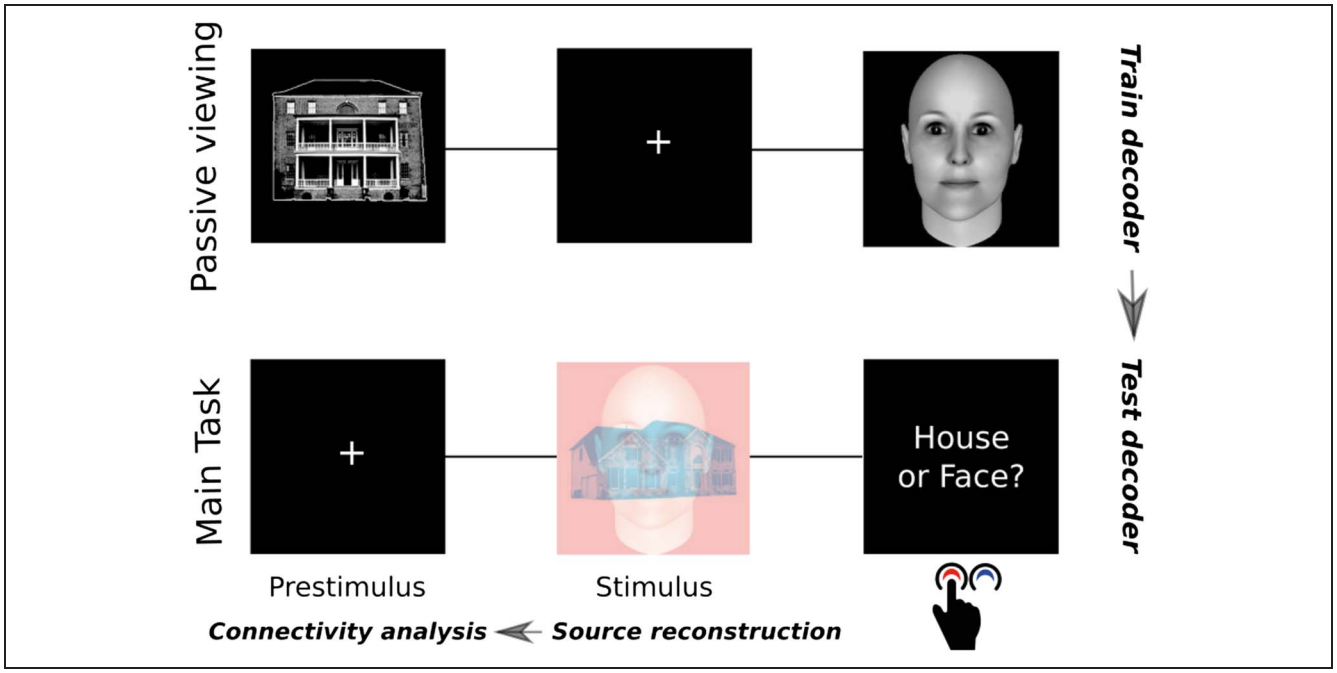

Figure 1. Experimental design. Example trial sequences from the passive viewing task where we trained the decoder (top) and the main experimental task where we tested the decoder (bottom).

with a right-handed button press to indicate their percept. The experiment consisted of six blocks of 80 trials each (a total of 480 trials).

MEG and MRI Data Acquisition

We recorded MEG using a 306-channel whole-head VectorView MEG system (Elekta-Neuromag, Ltd.; 204 gradiometers and 102 magnetometers) installed in a magnetically shielded chamber (AK3b, Vacuumschmelze), with signals recorded at a 1000-Hz sampling rate. We adjusted the hardware filters to band-pass the MEG signal in the frequency range of 0.01–330 Hz. Before the recording, we recorded points on the participant's head using a digitizer (Polhemus). These points included the five HPI coils, the three fiducials (nasion, left and right preauricular points), and around 300 additional points covering the head as evenly as possible. We used the HPI coils to monitor head position during the experiment.

We acquired structural T1-weigthed images with an magnetization prepared rapid gradient echo sequence (176 sagittal slices, repetition time = 2.7 sec, inversion time = 1020 msec, flip angle = 7°, 256 × 224 mm field of view, 1 × 1 × 1 mm resolution), using a 4-T magnetic MRI scanner (Bruker Biospin).

MEG Preprocessing and Source Projection

We preprocessed the data using the FieldTrip toolbox (Oostenveld, Fries, Maris, & Schoffelen, 2011). From the raw continuous data, we extracted epochs of 4 sec lasting from 2.5 sec before onset of the picture to 1.5 sec after stimulus onset. This resulted in 480 trials per participant. We applied a high-pass filter on this epoched data at 1 Hz (infinite impulse response Butterworth 6-order two-pass filter with 36-dB/octave roll-off), followed by a band-stop filter of 49–51 Hz to remove power line noise. We then down-sampled the data to 400 Hz. We visually inspected the trials for strong physiological (e.g., blinks) and non-physiological (e.g., channel jumps) artifacts and rejected the contaminated trials. For each participant, we then assigned the trials to the two conditions according to the participants' responses. Finally, we equalized the number of trials in each condition to ensure comparable signal-to-noise ratio, which left us with 182 trials per condition (364 in total) on average.

We projected the data to source space by applying LCMV (linear constrained mean variance) beamformer filters to the sensor-level data (Van Veen, van Drongelen, Yuchtman, & Suzuki, 1997). To create anatomically realistic head models (Nolte, 2003), we used structural MRI scans and the Polhemus digitized scalp shape. We used individual MRI scans for the five participants for which the scans were available, and for the rest, we used a template MRI that was morphed to fit the individuals' head shape using an affine transformation. We calculated a 3-D source grid (resolution: 8 mm) covering an entire Montreal Neurological Institute standard brain volume, aligned to the average of the head positions measured in between blocks. For each of these points, we computed an LCMV filter using the individual leadfield and the data covariance matrix. We then multiplied the sensor-level signal to the LCMV filters to obtain the time series for each source location in the grid and for each trial. Finally, we used a parcellation scheme of 333 parcels (Gordon et al., 2016) and averaged activity within each parcel.

To localize our ROI, we first calculated the time-locked averages of the parcellated source-level signals (band-pass filtered between 1 and 30 Hz), normalized the responses across participants, and baseline-corrected them with a relative baseline of −200 to 0 msec. We then computed the difference in the grand-averaged evoked responses between face and house trials (across participants and sources) to determine the time point at which there was the largest difference, which was at 165 msec. Finally, we contrasted face and house evoked response amplitude at that time point across participants with t statistics for each parcel source and chose the parcel with the largest t statistics as our ROI. As an additional, complementary analysis, we also localized individualized ROIs by selecting the parcel showing the largest difference in evoked responses per participant.

Multivariate Pattern Analysis Decoding

We performed multivariate pattern analysis (MVPA) decoding on the poststimulus period of 0–500 msec based on normalized (z-scored) single-trial sensor data down-sampled to 100 Hz and band-pass filtered between 0.1 and 40 Hz. We used MVPA as implemented in CoSMoMVPA (Oosterhof, Connolly, & Haxby, 2016) to identify when a common network between perception of unambiguous and rivalrous stimuli was activated. The two classes were face and house; in the rivalrous case, we labeled trials as face and house according to the participants' responses. The training set was the unambiguous trials, and the testing set was the rivalrous trials. We used a linear discriminant analysis classifier with the temporal generalization method (King & Dehaene, 2014) to assess the ability of the classifier across different time points in the training set to generalize to every time point in the testing set. We used local neighborhood features in time (in each time step of 10 msec, we included as additional features the previous and following time steps). We generated the time generalization matrix for each participant and statistically tested for above-chance decoding (defined as >50% accuracy) significance with a cluster-based permutation approach (clustering over the two time dimensions between 0 and 500 msec).

To calculate the difference in peak decoding latencies between training and testing data, we averaged the time-by-time spectrum across each of its two dimensions and identified the two time points at which these traces peaked, before subtracting them.

Analysis of Prestimulus Power, Graph Measures, and Coherence

We calculated spectral power, efficiency, the clustering coefficient in source-localized left FFA, as well as coherence between FFA and left V1 (defined by the parcellation scheme), in the prestimulus interval of −1 to 0 sec. We used multitaper frequency transformation with a spectral smoothing of 2 Hz to get Fourier coefficients. From those, we extracted power in FFA and computed coherence between FFA and V1.

For the graph analysis, we computed the cross-spectral density on source data and derived an all-to-all connectivity matrix of imaginary coherence, a conservative measure of phase synchronization. On the basis of nonzero phase differences, imaginary coherency capitalizes on out-of-phase interactions by removing instantaneous interactions, therefore eliminating the possibility that the interactions are because of field spread. So it measures a time-lagged component of connectivity, and high values indicate a consistent phase difference between sources (Bastos & Schoffelen, 2015).

After computing this value for All Sources × All Sources, we thresholded the resulting connectivity matrix to determine which sources were "neighbors," that is, adjacent to each other and having above-threshold imaginary coherency. We set the thresholds by taking the maximum value across the first dimension of the (Source × Source × Frequency × Time) connectivity matrix and then the minimum values of those maximum values across the second dimension of the matrix, obtaining a threshold per frequency and time point. Finally, we used the connectivity matrix and thresholded adjacency matrix to calculate local efficiency and local clustering coefficient in FFA. The local efficiency of FFA is the inverse of the average shortest path connecting all neighbors of FFA. The clustering coefficient is the probability that the neighbors of FFA are also connected to each other.

We averaged all of the above measures over the prestimulus time interval and contrasted face versus house estimates across participants with a cluster-based permutation approach.

Statistical Analysis

For all statistical analyses, we used nonparametric cluster permutation tests (Maris & Oostenveld, 2007), comparing a selected test statistic against a distribution obtained from 10,000 permutations. We set thresholds for forming clusters at $p < .05$ and considered an effect significant if its probability with respect to the nonparametric distribution was $p < .05$. For the evoked responses, we used two-sided dependent-samples t tests and clustered across the time dimension (0–500 msec). For the MVPA data, we used one-sided t tests (as we were interested in above-chance decoding) and clustered across the two time dimensions (both 0–500 msec). For the spectral power, efficiency, and clustering measures, we used one-sided t tests (as we hypothesized greater values for "face" trials) and clustered across the frequencies of 5–20 Hz. For the coherence measure, we did the same but clustered over the frequencies of 10–16 Hz. We used this restricted frequency range for this particular analysis because it is a replication of an analysis in our previous study (Rassi, Wutz, et al., 2019), which found this effect at those frequencies. For the correlations, we computed Pearson's coefficients.

RESULTS

Behavioral Reports Are Stochastic

We recorded whole-head MEG while 21 participants viewed an ambiguous image consisting of a red or blue face superimposed with a blue or red house. Participants wore red/blue glasses as we presented the image briefly and repeatedly and asked them to report the content of their percept (face or house) on each trial. That is, we used the typical binocular rivalry setup but with short presentation times such that only one percept is formed and then asked participants to report that percept (Figure 1, bottom: main task). Participants also passively viewed nonrivalrous versions of the face and house stimuli in a separate block before the main task (Figure 1, top: passive viewing).

To confirm that response choices in the main task were stochastic trial-by-trial, we binned consecutive responses in bins of 0–10 repetitions separately for face and house responses. We then averaged the number of repetitions in each bin across participants and fit these averaged values with a binomial distribution. The distribution accounted well for both face and house repetitions (goodness of fit: R^2 face = .92, R^2 house = .89). In other words, participants were equally likely to report "face" or "house" on each trial, regardless of their responses on previous trials. Overall, face reports constituted 40% of reports. For all subsequent analyses, we equalized the face and house trial numbers per participant by randomly omitting trials from the pool with more trials.

To investigate whether there were any biases arising from the dominance of one eye over the other, we looked at the proportion of responses corresponding to the right (covered by the red-filtered glass) eye versus the left (covered by the blue-filtered glass) eye and found that around 90% of responses were perceived with the right eye. This indicated that there was no serial dependency arising from a temporary dominance of one eye over the other but rather a strong bias likely arising from the right eye being consistently dominant over the left at rivalry onset.

Rivalry Resolution Is Delayed Compared to Nonrivalrous Vision

To explore the temporal dynamics of rivalry resolution, we first investigated the differences and similarities in neural

activity between perceiving a nonrivalrous face or house image and perceiving a face or house under binocular rivalry. For this purpose, we also recorded MEG while participants passively viewed a series of unambiguous, nonrivalrous face and house images before the main experiment. The motivation was twofold. First, we wanted to be confident that participants actually reported what they had perceived. Second, we wanted to investigate the time course for nonrivalrous versus rivalrous images. To achieve this, we used linear discriminant analysis to train a classifier on the broadband MEG signals resulting from the nonrivalrous images and tested it on the signals resulting from the rivalrous images using the temporal generalization method (King & Dehaene, 2014).

The classifier performed significantly above chance in the poststimulus period (0–500 msec; p[cluster] < .001), meaning that the nonrivalrous and rivalrous conditions shared decodable neural representations (Figure 2A). The signals from the nonrivalrous data at 85 msec onwards could significantly predict those of the rivalrous data from 120 msec onwards. Decoding accuracy peaked outside the diagonal of the time generalization matrix, indicating a delay in decodability. To quantify this delay, we calculated the difference between the time at which the nonrivalrous data could most predict the rivalrous data and the time at which the rivalrous data could most predict the nonrivalrous data (Figure 2B). The difference between these two latencies was, on average, 36 msec (SD = 30 msec, range = −5 to 130 msec), and it was significant (t = 6.8, p < .0001). Overall, this analysis gave us confidence that participants truly reported what they had perceived and showed that visual content is decodable from brain responses to ambiguous and unambiguous stimuli. More importantly, this result indicates that, when faced with a bistable face–house stimulus, the brain requires approximately an additional 36 msec to resolve this ambiguity.

Differences in Evoked Responses Were Localized in the Left Fusiform Gyrus

To answer our main question of whether prestimulus activity in category-sensitive brain regions biases upcoming perceptual content, we first defined such a region in a data-driven manner. We used a beamforming approach to project our data to source space and grand-averaged the evoked responses to faces and houses across sources and participants (Figure 2D). The difference between the two evoked responses was significant during the poststimulus period (0–500 msec). The difference was pronounced in two clusters, a positive cluster (face > house; 157–165 msec; p[cluster] =. 010) and a negative cluster (house > face; 305–333 msec; p[cluster] = .012). The difference peaked 165 msec after stimulus onset, in a similar time window in which the MVPA classifier achieved

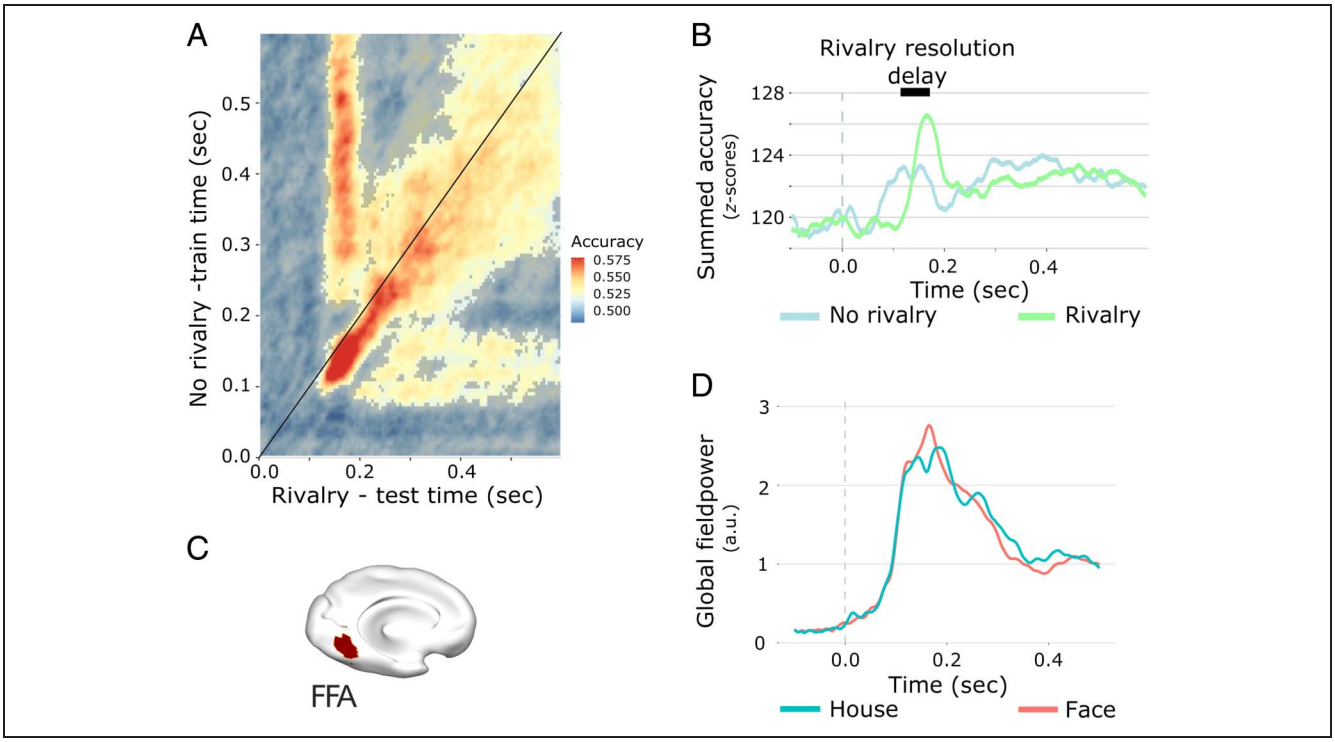

Figure 2. Poststimulus responses to rivalrous and nonrivalrous face/house images. (A) Face versus house decoding of sensor-level data using the time-by-time generalization method, obtained from training a classifier on evoked responses to unambiguous face and house images, and testing on evoked responses to the bistable face/house images. (B) Peak decoding accuracy of the rivalrous data was around 36 msec later than the time of peak decoding accuracy of the nonrivalrous data. Blue line represents the accuracy z score summed over each row of A. Green line represents the accuracy z score summed over each column of A. (C) Source-localized ROI: FFA. (D) Global field power (event-related fields) in source space (averaged across all voxels).

peak decodability. We then defined our ROI as the region where this difference was strongest. Perhaps inconsistent with previous literature (Kanwisher, McDermott, & Chun, 1997), we localized the difference in responses to faces and houses in the left (rather than the right) fusiform gyrus (Figure 2C, FFA; Montreal Neurological Institute coordinates: [−28, −58, −8] mm). For the subsequent analyses, we used left FFA as our ROI. However, we also localized FFA on an individual basis such as to replicate the main results we would get from using the group-averaged left FFA. The activations were all bilateral with small degrees of lateralization. Of 21 participants, the responses of eight (of which two were left-handed) were localized in the left fusiform gyrus; and those of the remaining 13 (of which one was left-handed), in the right fusiform gyrus.

To further make sure that we had chosen the correct ROI, we computed the event-related fields in left FFA for face and house reports in the main task (Figure 3A) as well as for right FFA. For descriptive purposes, we also computed the event-related fields in left FFA for face and house reports in the passive viewing task (Figure 3B). We then took the difference in field power at the time point where the difference was maximal in the main task, at 165 msec, for both left and right FFA. The differences in left FFA were slightly larger than those in right FFA (Figure 3C; $t = 0.15$, $p > .5$), and their standard deviation was less (left FFA: $SD = 3.6$; right FFA: $SD = 7.9$). Overall, we were confident that left FFA was the region that was most sensitive to our task and stimuli.

Prestimulus Connectivity Biases Perceptual Report

Next, we investigated whether oscillatory power and connectivity in FFA were different before the participants reported "face" versus "house." We used a nonparametric cluster-based permutation approach (Maris & Oostenveld, 2007) to correct for multiple comparisons over the 5- to 20-Hz frequency range. The frequency spectra from both trial types showed that oscillatory activity was largely restricted to the 5- to 20-Hz range, with clear alpha-band peaks around 10 Hz. However, we found no statistical differences in prestimulus power between face and house trials (Figure 4A). This finding is consistent with our recent similar study, which reported increased connectivity

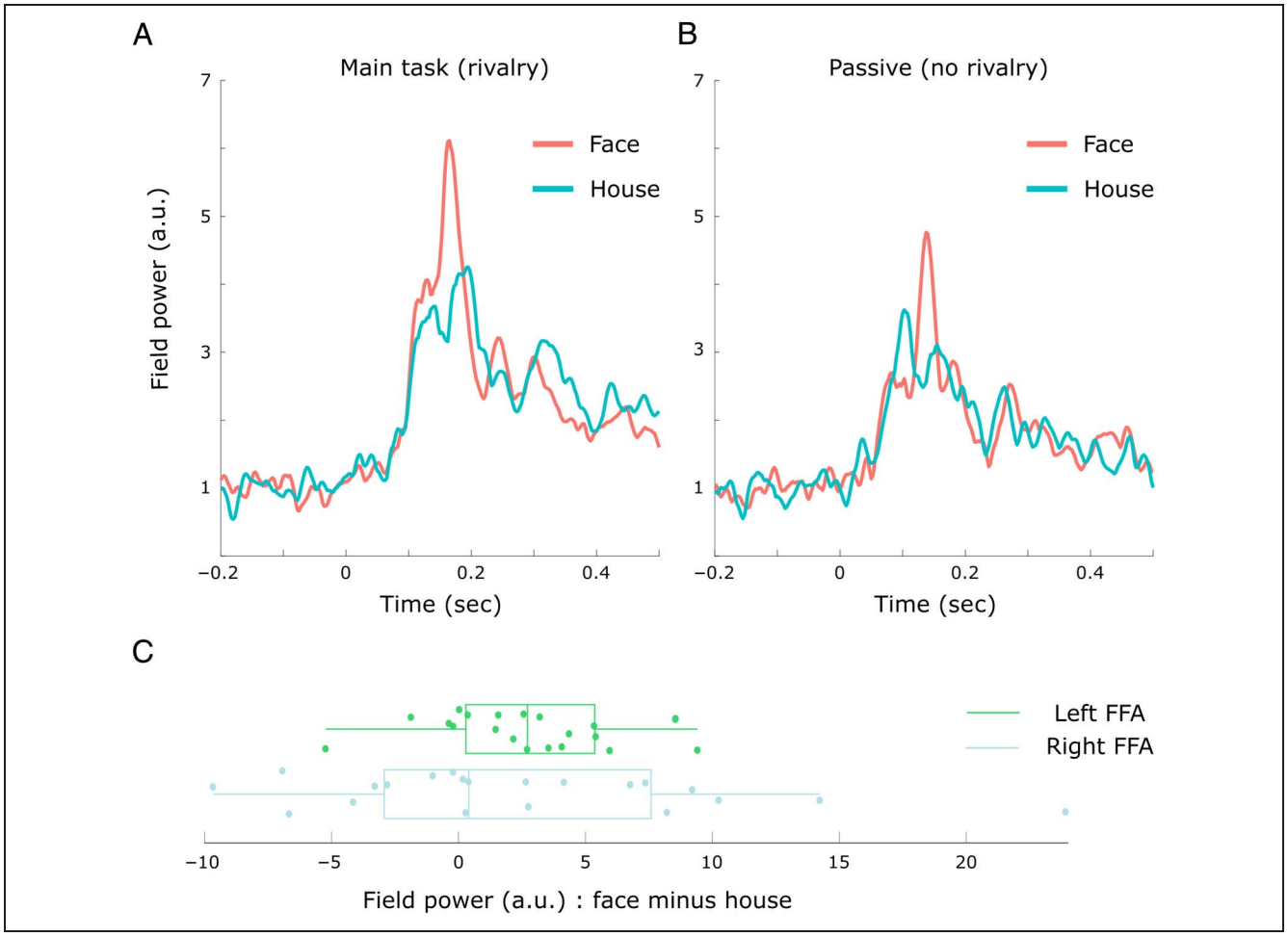

Figure 3. Differences in event-related fields were maximal in left FFA. (A) Event-related fields for face versus house trials, in left FFA during the main task. (B) Event-related fields for face versus house trials, in left FFA during the passive viewing task. (C) Differences in face versus house event-related fields at 165 msec, in both left and right FFA during the main task.

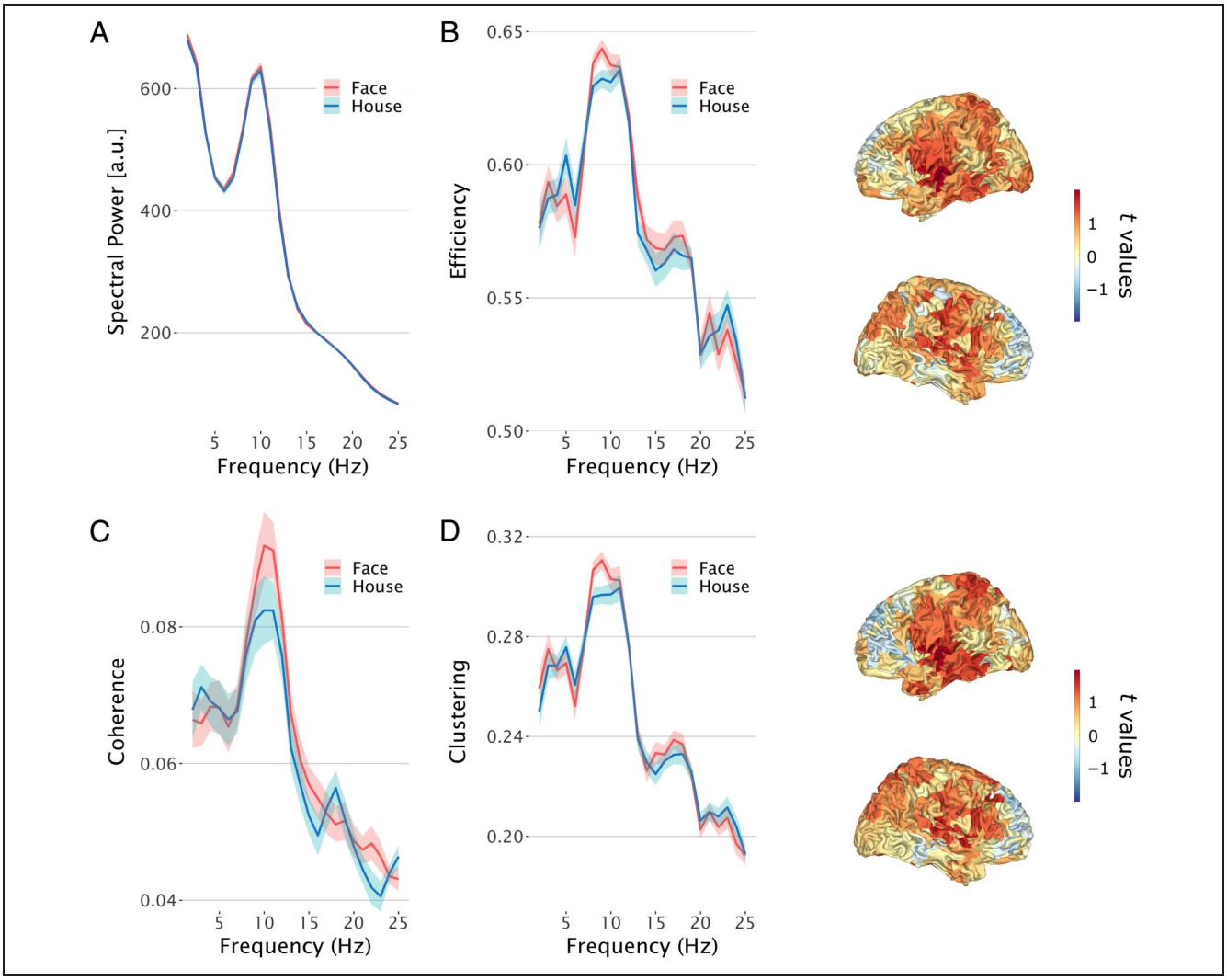

Figure 4. Prestimulus MEG connectivity biases upcoming perception. Line graphs based on source data averaged within FFA. Shaded areas represent the *SEM*. (A) No difference in prestimulus spectral power between face and house trials in FFA. (B) Left: prestimulus efficiency in FFA was increased on face trials compared to house trials. Right: whole-brain map of face versus house efficiency t values. (C) Prestimulus coherence between V1 and FFA was increased on face trials compared to house trials. (D) Left: prestimulus clustering in FFA was increased on face trials compared to house trials. Right: whole-brain map of face versus house clustering t values.

between FFA and primary visual cortex (V1) before face reports, despite no differences in power (Rassi, Wutz, et al., 2019). We therefore additionally investigated the prestimulus coherence between FFA and atlas-defined (left-hemisphere) V1. We calculated coherence in a frequency-resolved manner and used a cluster-based permutation approach to contrast prestimulus coherence between FFA and V1 on face versus house trials. Here, we restricted our statistical testing to the frequency range in which the aforementioned study reported the coherence effect (10–16 Hz). We found increased prestimulus coherence in the alpha range on face (vs. house) trials (p[cluster] = .021; Figure 4C). We also repeated the same analysis between FFA and opposite-hemisphere (right) V1 and found increased coherence on face (vs. house) trials, but this effect was not significant (p = .08).

In summary, consistent with the aforementioned study, FFA and V1 were more strongly connected before face (vs. house) responses, despite no differences in power between the two trial types. Crucially, this meant that connectivity effects would not be confounded with power differences in the current data set.

In the next step, we investigated whether the network integration patterns of FFA influence the perceptual reports. To assess this information, we applied two local graph theoretical measures to thresholded (i.e., binary) connectivity matrices. The first was local efficiency, a measure of how well integrated a node is to the rest of the network estimated by the inverse of the average shortest path from this node to all other network nodes. The second was the local clustering coefficient, a measure of the robustness of the region's local network (i.e., the probability that nodes to which the region is connected are connected among each other). We computed these measures in a frequency-resolved manner and used a cluster-based permutation approach (clustering over

the frequencies of 5–20 Hz) to contrast prestimulus efficiency and clustering of FFA between face and house trials. We found that FFA showed increased prestimulus efficiency and clustering on face trials compared to house trials (Figure 4B, efficiency: p[cluster] = .017; Figure 4D, clustering: p[cluster] = .024), despite no differences in spectral power. In both cases, the difference was most pronounced in the alpha band, particularly at frequencies of 8–9 Hz. We additionally replicated these results using the individually defined (rather than group-averaged) ROIs by testing at the frequencies of 8 and 9 Hz and again found increased prestimulus efficiency and clustering on face trials compared to house trials (efficiency: t[cluster] = 2.27, p = .036; clustering: t[cluster] = 2.24, p = .037).

In summary, FFA was more efficiently connected to the rest of the brain in a robust manner before face (vs. house) responses.

Prestimulus Connectivity Predicts Poststimulus Decoding Accuracy and Rivalry Resolution

Finally, we investigated whether prestimulus connectivity predicts poststimulus category-related and rivalry-related neural activity across participants. For each participant, we extracted the maximum face versus house decoding accuracy and the average rivalry-related delay in decodability from the time generalization results as well as the average differences between face and house trials in prestimulus efficiency and clustering. Maximum decoding accuracy was positively correlated with both the prestimulus efficiency (Figure 5A; r = .55, p = .010) and prestimulus clustering (Figure 5B; r = .59, p = .005) differences. In other words, participants who showed stronger prestimulus connectivity effects also showed more robust poststimulus decoding. Consequently, in addition to being predictive of upcoming perceptual reports, prestimulus

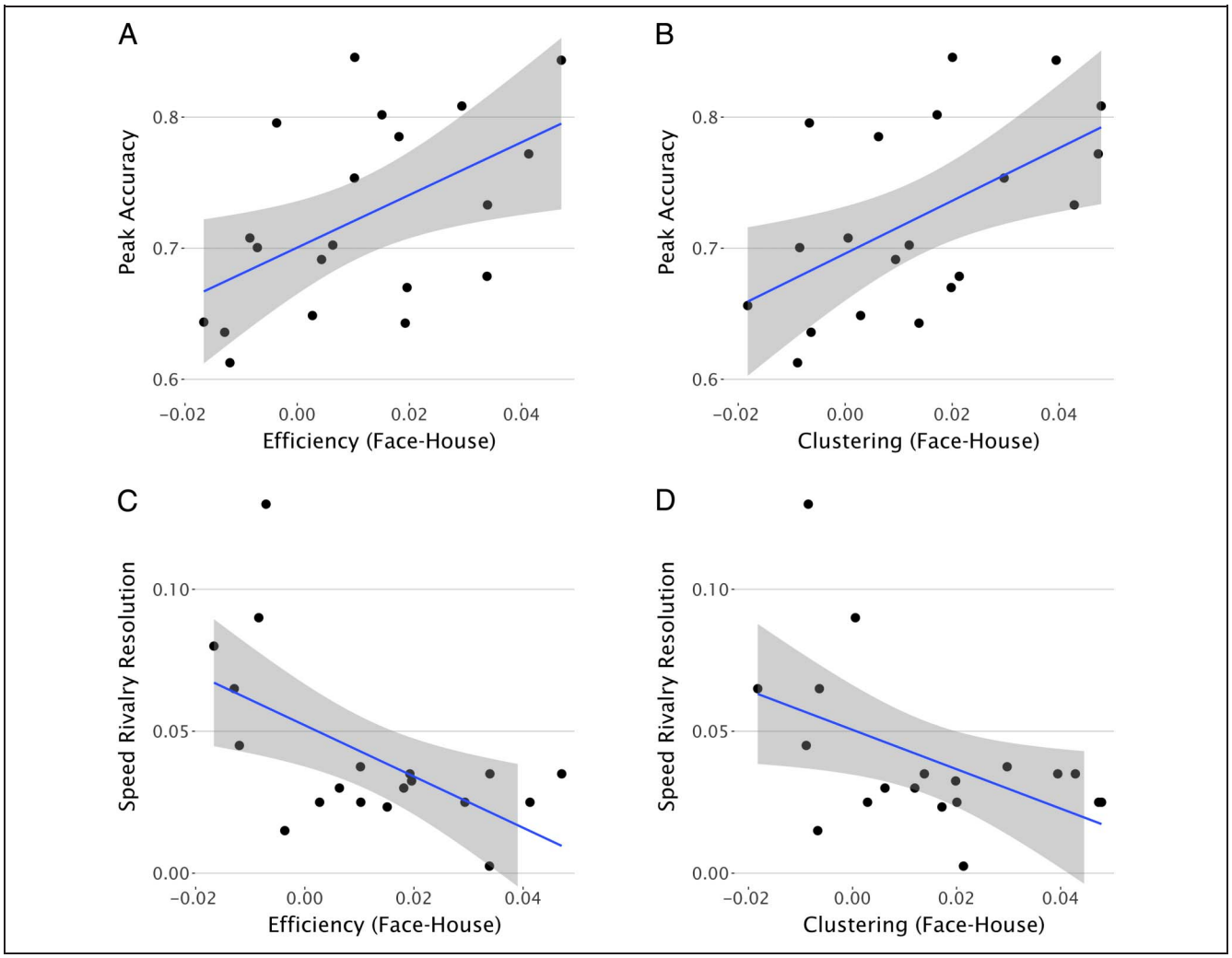

Figure 5. Prestimulus connectivity is correlated with poststimulus decoding accuracy and rivalry resolution across participants. r Values represent Pearson's correlation coefficients. Shaded areas represent 95% confidence intervals. (A) Mean prestimulus efficiency differences are correlated with maximum poststimulus decoding accuracy. (B) Mean prestimulus clustering differences are correlated with maximum poststimulus decoding accuracy. (C) Mean prestimulus efficiency differences are negatively correlated with speed of rivalry resolution. (D) Mean prestimulus clustering differences are negatively correlated with speed of rivalry resolution.

connectivity was also predictive of the strength of poststimulus signals associated with those percepts.

Furthermore, the rivalry-related delay in poststimulus decoding was negatively correlated with both the prestimulus efficiency (Figure 5C; $r = -.50$, $p = .022$) and prestimulus clustering (Figure 5D; $r = -.53$, $p = .013$) differences. In other words, participants who showed stronger prestimulus effects also had shorter delays in poststimulus rivalry decodability. Overall, these results indicate that the influence of prestimulus connectivity on poststimulus neural signals is manifested in higher decoding accuracy and shorter delays in rivalry resolution.

DISCUSSION

Although the prestimulus requisites of near-threshold conscious perception have been widely studied (Benwell et al., 2017; Iemi et al., 2017; Frey et al., 2016; Leonardelli et al., 2015; Leske et al., 2015; Weisz et al., 2014; Sadaghiani et al., 2009; Boly et al., 2007; Hanslmayr et al., 2007; Ergenoglu et al., 2004), very few studies have investigated the influence of prestimulus activity on object perception (Gandolfo & Downing, 2019; Hesselmann et al., 2008). These fMRI studies reported increased activity in category-selective extrastriate regions before object perception, but these prestimulus BOLD activations could represent increased local excitability of a cortical region, or they could be a product of increased connectedness of that region. In fact, in our recent MEG study, we reported that increased prestimulus connectivity between striate and extrastriate regions, but not local excitability of these regions, predicted upcoming object perception (Rassi, Wutz, et al., 2019), a finding that we replicate in the current study.

Here, we aimed to add to this emerging literature by employing a paradigm similar to the one in the aforementioned MEG study and investigating possible influences of prestimulus excitability and connectivity on object perception in a binocular rivalry setup. The rationale was to investigate whether a similar pattern of results would emerge under binocular rivalry, where ambiguity is likely resolved in the brain differently than it would be with a single ambiguous image (e.g., ocular dominance columns might be involved in resolving binocular rivalry but not the Rubin face/vase illusion). In other words, we wanted to check that our previous results were robust to changes in the way the stimuli are perceived at a low level. The current design further allowed us to investigate the rivalry-related delay in perceiving the binocular stimulus versus the same or very similar unambiguous versions of the stimulus, which would not have been possible with the Rubin vase stimulus. In addition, whereas our previous study dealt with the connectivity between only two ROIs (FFA and V1), the focus of the current study was on the graph theoretical connectivity analyses, which account for connectivity at the whole-brain level.

Whereas our previous study, as well as the literature on FFA lateralization (Bukowski, Dricot, Hanseeuw, & Rossion, 2013; Willems, Peelen, & Hagoort, 2010; Kanwisher et al., 1997), localized FFA in the right hemisphere (except for left-handed participants), here our data-driven, group-averaged approach localized it in the left fusiform gyrus. We note that our goal was not to localize FFA specifically but rather to find the brain region that was most sensitive to our particular task. A possible reason for this discrepancy is that, although most FFA studies have contrasted face images with scrambles faces, body parts, or other objects, here we contrasted face and house images. It is possible that, given the closeness of the face and place areas near the right fusiform gyrus, and given the resolution of MEG source reconstruction, a contrast between face and house trials cancels out differences in the right fusiform gyrus, yielding a more pronounced difference in the left hemisphere. Ultimately, we decided to use our group-averaged ROI such that the approach is consistent with that of our previous study. However, to preclude this as a limitation, we also replicated the finding using individually localized ROIs.

To recap, we showed people a bistable face/house image whose perceptual content would vary trial-by-trial and asked them to report their percept on each trial. We source-localized the poststimulus activity to FFA and subsequently focused on differences between face-report and house-report trials in prestimulus FFA activity. We found no differences in FFA oscillatory alpha-band power before trials perceived as face versus house. Nevertheless, we did observe differences in FFA connectivity states before trials perceived as face versus house. Specifically, FFA was more efficiently and robustly connected to the rest of cortex in the alpha frequency range before face (vs. house) perception of the bistable face/house image. These connectivity differences were correlated with poststimulus decoding accuracy and speed of rivalry resolution across participants.

The prestimulus connectivity results of this study were in the alpha band. Alpha oscillations are implicated in a variety of cognitive and perceptual phenomena (Klimesch, 2012) and act on neuronal populations by rhythmic inhibition (Haegens, Nácher, Luna, Romo, & Jensen, 2011). Their power can therefore be thought of as a proxy to neural excitability. If the prestimulus levels of excitation per se of the task-relevant sensory cortices influenced upcoming object perception, we would expect prestimulus alpha power in FFA to be different on face versus house trials. Yet, we did not observe such a difference. Despite this, we found differences between face and house trials in the prestimulus connectivity states of FFA. Although prestimulus excitability of task-relevant sensory cortices influences simpler perceptual operations such as near-threshold detection (Zazio, Ruhnau, Weisz, & Wutz, 2021; Iemi & Busch, 2018), our findings indicate that the connectivity states of these task-relevant regions are more relevant to understanding more complex perceptual operations, such as visual object perception.

Graph theoretical measures of network connectivity have provided important insights into properties of structural and functional brain networks, such as small-worldness and the existence of hubs (Peatfield, Choi, & Weisz, 2016; Bullmore & Sporns, 2009). Here, we used the graph theoretical measures of efficiency and clustering coefficient to inform us about the connectivity states of FFA before face and house perception. We found increased prestimulus local efficiency in FFA on face (vs. house) trials. This means that FFA was more highly integrated into the rest of the network before face (vs. house) perception. In other words, when FFA was better integrated in cortex, people were more likely to subsequently perceive a face rather than a house. We additionally found increased prestimulus local clustering in FFA on face (vs. house) trials. This means that FFA was more densely connected to its neighbors before face (vs. house) perception. In other words, when the network to which FFA belongs was more robust, participants were more likely to subsequently perceive a face rather than a house.

Our results provide further support to the Windows to Consciousness framework (Ruhnau et al., 2014; Weisz et al., 2014), which postulates that ongoing neural fluctuations impact preestablished connectivity pathways and influence upcoming perception. We now widen this view to include object perception, which is known to involve ventral stream activity, especially in the case of stimuli with semantic content. Because our time generalization decoding analysis supported the notion that ambiguous and unambiguous perceptions share common neural substrates, we hypothesized that the ventral visual pathway can be the candidate preestablished connectivity pathway. In support of this hypothesis, we found increased coherence between V1 and FFA before face (vs. house) perception.

Given that our effects are in the alpha band, known to be inhibitory, it is possible that the increased connectivity between V1 and FFA here reflects the suppression of the irrelevant signal rather than the boosting of the relevant signal. Because V1 has representations of each eye, which are competing in rivalry, this remains a plausible alternative explanation. Our data cannot disentangle which of the two interpretations is more likely as ocular dominance columns are beyond the spatial resolution of MEG. However, we have shown this same pattern in a study where the stimulus was a bistable face/vase image, but no ocular dominance or binocular rivalry was involved, so it seems more likely that the signal is being enhanced rather than suppressed via this connectivity pathway.

Despite the similarity in neural responses to rivalrous and nonrivalrous images, we found an important difference between them. Decoding of responses to the rivalrous images was delayed with respect to those of the nonrivalrous images. This possibly relates to a delay in disambiguating the bistable image, before perceptual content becomes consciously accessible. In other words, this delay can be thought of as representing the speed at which rivalry is resolved on average within a participant. In fact, this delay was negatively correlated with the prestimulus connectivity effects, indicating that participants showing stronger connectivity effects also resolved the binocular rivalry faster. Finally, we reasoned that if prestimulus connectivity biases upcoming object perception, then it should also bias the poststimulus signals associated with object perception. We found that both prestimulus efficiency and clustering correlated well with face versus house decoding accuracy scores. The stronger the prestimulus effect was, the more decodable the poststimulus signals were. This could indicate that participants who were more prone to the prestimulus connectivity effects were also better at subsequently disambiguating the bistable stimulus. Overall, it appears that prestimulus connectivity biases not only perceptual contents but also the strength and speed of content-related neural activity.

It is difficult to assign cognitive functions to the connectivity effects we detected, but at least two interpretations of these effects are plausible. One is that a conscious, top–down drive to perceive one of the contents of the stimuli leads to increased connectivity of the relevant cortical region, which in turn biases perception. This interpretation is in line with a large body of literature suggesting that expectations, predictions, or context critically shapes perception (de Lange, Heilbron, & Kok, 2018; Battistoni, Stein, & Peelen, 2017; Kok, Jehee, & de Lange, 2012; Summerfield & Egner, 2009). That the effects were in the alpha frequencies might also support this interpretation, given the evidence from human and nonhuman primate studies showing that alpha oscillations subserve feedback connectivity in visual cortical areas (Bastos et al., 2015; van Kerkoerle et al., 2014). However, a purely top–down interpretation is unlikely given our design and behavioral analysis: The prestimulus intervals were short (1–2 sec), and stimulus onset was jittered and difficult to predict within this range; in addition, our behavioral analysis indicated that the response sequences were stochastic. Therefore, the other plausible interpretation is that spontaneous fluctuations in neural activity, which could randomly differ on a trial-by-trial basis, influence the connectivity state of the relevant cortical region and, in turn, bias perception.

Acknowledgments

We thank Anne Hauswald, Chrysa Lithari, and Gaëtan Sanchez, Gianpaolo Demarchi, and Thomas Hartmann for assistance and valuable input on data analysis.

Reprint requests should be sent to Elie Rassi, Donders Institute for Brain Cognition and Behaviour, Radboud University, Kapittelweg 29, Nijmegen, Gelderland 6500 GL, The Netherlands, or via e-mail: elie.r.rassi@gmail.com.

Author Contributions

Elie Rassi: Conceptualization; Investigation; Methodology; Visualization; Writing—Original draft. Andreas Wutz:

Supervision; Writing—Review & editing. Nicholas Peatfield: Conceptualization; Investigation; Methodology; Supervision; Writing—Review & editing. Nathan Weisz: Conceptualization; Methodology; Supervision; Writing—Review & editing.

Funding Information

This work was funded by FWF Austrian Science Fund, Imaging the Mind: Connectivity and Higher Cognitive Function grant W 1233-G17 (E. R.), FWF Lise Meitner fellowship M02496 (A. W.), and European Research Council grant WIN2CON, ERC StG 283404 (N. W.).

Data and Materials Availability

The data and code used in the analysis are publicly available at https://osf.io/fptz9/.

Diversity in Citation Practices

Retrospective analysis of the citations in every article published in this journal from 2010 to 2021 reveals a persistent pattern of gender imbalance: Although the proportions of authorship teams (categorized by estimated gender identification of first author/last author) publishing in the *Journal of Cognitive Neuroscience* (*JoCN*) during this period were M(an)/M = .407, W(oman)/M = .32, M/W = .115, and W/W = .159, the comparable proportions for the articles that these authorship teams cited were M/M = .549, W/M = .257, M/W = .109, and W/W = .085 (Postle and Fulvio, *JoCN*, 34:1, pp. 1–3). Consequently, *JoCN* encourages all authors to consider gender balance explicitly when selecting which articles to cite and gives them the opportunity to report their article's gender citation balance.

REFERENCES

Abdallah, D., & Brooks, J. L. (2020). Response dependence of reversal-related ERP components in perception of ambiguous figures. *Psychophysiology*, *57*, e13685. https://doi.org/10.1111/psyp.13685, PubMed: 32940372

Başar, E., Gönder, A., & Ungan, P. (1976). Important relation between EEG and brain evoked potentials. *Biological Cybernetics*, *25*, 41–48. https://doi.org/10.1007/BF00337047, PubMed: 999965

Bastos, A. M., & Schoffelen, J.-M. (2015). A tutorial review of functional connectivity analysis methods and their interpretational pitfalls. *Frontiers in Systems Neuroscience*, *9*, 175. https://doi.org/10.3389/fnsys.2015.00175, PubMed: 26778976

Bastos, A. M., Vezoli, J., Bosman, C. A., Schoffelen, J.-M., Oostenveld, R., Dowdall, J. R., et al. (2015). Visual areas exert feedforward and feedback influences through distinct frequency channels. *Neuron*, *85*, 390–401. https://doi.org/10.1016/j.neuron.2014.12.018, PubMed: 25556836

Battistoni, E., Stein, T., & Peelen, M. V. (2017). Preparatory attention in visual cortex. *Annals of the New York Academy of Sciences*, *1396*, 92–107. https://doi.org/10.1111/nyas.13320, PubMed: 28253445

Benwell, C. S. Y., Tagliabue, C. F., Veniero, D., Cecere, R., Savazzi, S., & Thut, G. (2017). Prestimulus EEG power predicts conscious awareness but not objective visual performance. *eNeuro*, *4*. https://doi.org/10.1523/ENEURO.0182-17.2017, PubMed: 29255794

Boly, M., Balteau, E., Schnakers, C., Degueldre, C., Moonen, G., Luxen, A., et al. (2007). Baseline brain activity fluctuations predict somatosensory perception in humans. *Proceedings of the National Academy of Sciences, U.S.A.*, *104*, 12187–12192. https://doi.org/10.1073/pnas.0611404104, PubMed: 17616583

Brascamp, J., Sterzer, P., Blake, R., & Knapen, T. (2018). Multistable perception and the role of the frontoparietal cortex in perceptual inference. *Annual Review of Psychology*, *69*, 77–103. https://doi.org/10.1146/annurev-psych-010417-085944, PubMed: 28854000

Bukowski, H., Dricot, L., Hanseeuw, B., & Rossion, B. (2013). Cerebral lateralization of face-sensitive areas in left-handers: Only the FFA does not get it right. *Cortex*, *49*, 2583–2589. https://doi.org/10.1016/j.cortex.2013.05.002, PubMed: 23906596

Bullmore, E., & Sporns, O. (2009). Complex brain networks: Graph theoretical analysis of structural and functional systems. *Nature Reviews Neuroscience*, *10*, 186–198. https://doi.org/10.1038/nrn2575, PubMed: 19190637

de Lange, F. P., Heilbron, M., & Kok, P. (2018). How do expectations shape perception? *Trends in Cognitive Sciences*, *22*, 764–779. https://doi.org/10.1016/j.tics.2018.06.002, PubMed: 30122170

Ergenoglu, T., Demiralp, T., Bayraktaroglu, Z., Ergen, M., Beydagi, H., & Uresin, Y. (2004). Alpha rhythm of the EEG modulates visual detection performance in humans. *Cognitive Brain Research*, *20*, 376–383. https://doi.org/10.1016/j.cogbrainres.2004.03.009, PubMed: 15268915

Frey, J. N., Ruhnau, P., Leske, S., Siegel, M., Braun, C., & Weisz, N. (2016). The tactile window to consciousness is characterized by frequency-specific integration and segregation of the primary somatosensory cortex. *Scientific Reports*, *6*, 20805. https://doi.org/10.1038/srep20805, PubMed: 26864304

Gandolfo, M., & Downing, P. E. (2019). Causal evidence for expression of perceptual expectations in category-selective extrastriate regions. *Current Biology*, *29*, 2496–2500. https://doi.org/10.1016/j.cub.2019.06.024, PubMed: 31327721

Gordon, E. M., Laumann, T. O., Adeyemo, B., Huckins, J. F., Kelley, W. M., & Petersen, S. E. (2016). Generation and evaluation of a cortical area parcellation from resting-state correlations. *Cerebral Cortex*, *26*, 288–303. https://doi.org/10.1093/cercor/bhu239, PubMed: 25316338

Haegens, S., Nácher, V., Luna, R., Romo, R., & Jensen, O. (2011). α-Oscillations in the monkey sensorimotor network influence discrimination performance by rhythmical inhibition of neuronal spiking. *Proceedings of the National Academy of Sciences, U.S.A.*, *108*, 19377–19382. https://doi.org/10.1073/pnas.1117190108, PubMed: 22084106

Hanslmayr, S., Aslan, A., Staudigl, T., Klimesch, W., Herrmann, C. S., & Bäuml, K.-H. (2007). Prestimulus oscillations predict visual perception performance between and within subjects. *Neuroimage*, *37*, 1465–1473. https://doi.org/10.1016/j.neuroimage.2007.07.011, PubMed: 17706433

Hasson, U., Hendler, T., Bashat, D. B., & Malach, R. (2001). Vase or face? A neural correlate of shape-selective grouping processes in the human brain. *Journal of Cognitive Neuroscience*, *13*, 744–753. https://doi.org/10.1162/08989290152541412, PubMed: 11564319

Hesselmann, G., Kell, C. A., Eger, E., & Kleinschmidt, A. (2008). Spontaneous local variations in ongoing neural activity bias perceptual decisions. *Proceedings of the National Academy*

of Sciences, U.S.A., *105*, 10984–10989. https://doi.org/10.1073/pnas.0712043105, PubMed: 18664576

Iemi, L., & Busch, N. A. (2018). Moment-to-moment fluctuations in neuronal excitability bias subjective perception rather than strategic decision-making. *eNeuro*, *5*. https://doi.org/10.1523/ENEURO.0430-17.2018, PubMed: 29911179

Iemi, L., Chaumon, M., Crouzet, S. M., & Busch, N. A. (2017). Spontaneous neural oscillations bias perception by modulating baseline excitability. *Journal of Neuroscience*, *37*, 807–819. https://doi.org/10.1523/JNEUROSCI.1432-16.2016, PubMed: 28123017

Jensen, O., & Mazaheri, A. (2010). Shaping functional architecture by oscillatory alpha activity: Gating by inhibition. *Frontiers in Human Neuroscience*, *4*, 186. https://doi.org/10.3389/fnhum.2010.00186, PubMed: 21119777

Kanwisher, N., McDermott, J., & Chun, M. M. (1997). The fusiform face area: A module in human extrastriate cortex specialized for face perception. *Journal of Neuroscience*, *17*, 4302–4311. https://doi.org/10.1523/JNEUROSCI.17-11-04302.1997, PubMed: 9151747

King, J.-R., & Dehaene, S. (2014). Characterizing the dynamics of mental representations: The temporal generalization method. *Trends in Cognitive Sciences*, *18*, 203–210. https://doi.org/10.1016/j.tics.2014.01.002, PubMed: 24593982

Kleiner, M., Brainard, D., Pelli, D., Ingling, A., Murray, R., & Broussard, C. (2007). What's new in psychtoolbox-3. *Perception*, *36*, 1–16.

Klimesch, W. (2012). α-Band oscillations, attention, and controlled access to stored information. *Trends in Cognitive Sciences*, *16*, 606–617. https://doi.org/10.1016/j.tics.2012.10.007, PubMed: 23141428

Klimesch, W., Sauseng, P., & Hanslmayr, S. (2007). EEG alpha oscillations: The inhibition–timing hypothesis. *Brain Research Reviews*, *53*, 63–88. https://doi.org/10.1016/j.brainresrev.2006.06.003, PubMed: 16887192

Kok, P., Jehee, J. F. M., & de Lange, F. P. (2012). Less is more: Expectation sharpens representations in the primary visual cortex. *Neuron*, *75*, 265–270. https://doi.org/10.1016/j.neuron.2012.04.034, PubMed: 22841311

Leonardelli, E., Braun, C., Weisz, N., Lithari, C., Occelli, V., & Zampini, M. (2015). Prestimulus oscillatory alpha power and connectivity patterns predispose perceptual integration of an audio and a tactile stimulus. *Human Brain Mapping*, *36*, 3486–3498. https://doi.org/10.1002/hbm.22857, PubMed: 26109518

Leopold, D. A., & Logothetis, N. K. (1996). Activity changes in early visual cortex reflect monkeys' percepts during binocular rivalry. *Nature*, *379*, 549–553. https://doi.org/10.1038/379549a0, PubMed: 8596635

Leske, S., Ruhnau, P., Frey, J., Lithari, C., Müller, N., Hartmann, T., et al. (2015). Prestimulus network integration of auditory cortex predisposes near-threshold perception independently of local excitability. *Cerebral Cortex*, *25*, 4898–4907. https://doi.org/10.1093/cercor/bhv212, PubMed: 26408799

Logothetis, N. K., & Sheinberg, D. L. (1996). Visual object recognition. *Annual Review of Neuroscience*, *19*, 577–621. https://doi.org/10.1146/annurev.ne.19.030196.003045, PubMed: 8833455

Maris, E., & Oostenveld, R. (2007). Nonparametric statistical testing of EEG- and MEG-data. *Journal of Neuroscience Methods*, *164*, 177–190. https://doi.org/10.1016/j.jneumeth.2007.03.024, PubMed: 17517438

Miller, E. K., Nieder, A., Freedman, D. J., & Wallis, J. D. (2003). Neural correlates of categories and concepts. *Current Opinion in Neurobiology*, *13*, 198–203. https://doi.org/10.1016/S0959-4388(03)00037-0, PubMed: 12744974

Necker, L. A. (1832). LXI. Observations on some remarkable optical phænomena seen in Switzerland; and on an optical phænomenon which occurs on viewing a figure of a crystal or geometrical solid. *The London, Edinburgh, and Dublin Philosophical Magazine and Journal of Science*, *1*, 329–337. https://doi.org/10.1080/14786443208647909

Nolte, G. (2003). The magnetic lead field theorem in the quasi-static approximation and its use for magnetoencephalography forward calculation in realistic volume conductors. *Physics in Medicine and Biology*, *48*, 3637–3652. https://doi.org/10.1088/0031-9155/48/22/002, PubMed: 14680264

Oostenveld, R., Fries, P., Maris, E., & Schoffelen, J.-M. (2011). FieldTrip: Open source software for advanced analysis of MEG, EEG, and invasive electrophysiological data. *Computational Intelligence and Neuroscience*, *2011*, 156869. https://doi.org/10.1155/2011/156869, PubMed: 21253357

Oosterhof, N. N., Connolly, A. C., & Haxby, J. V. (2016). CoSMoMVPA: Multi-modal multivariate pattern analysis of neuroimaging data in MATLAB/GNU octave. *Frontiers in Neuroinformatics*, *10*, 27. https://doi.org/10.3389/fninf.2016.00027, PubMed: 27499741

Panagiotaropoulos, T. I., Dwarakanath, A., & Kapoor, V. (2020). Prefrontal cortex and consciousness: Beware of the signals. *Trends in Cognitive Sciences*, *24*, 343–344. https://doi.org/10.1016/j.tics.2020.02.005, PubMed: 32298618

Peatfield, N. A., Choi, D., & Weisz, N. (2016) Dynamical network states as predisposition of perception. In S. Palva (Ed.), *Multimodal oscillation-based connectivity theory* (pp. 19–27). Cham, Switzerland: Springer International Publishing. https://doi.org/10.1007/978-3-319-32265-0_2

Pitts, M. A., Martínez, A., Brewer, J. B., & Hillyard, S. A. (2011). Early stages of figure–ground segregation during perception of the face–vase. *Journal of Cognitive Neuroscience*, *23*, 880–895. https://doi.org/10.1162/jocn.2010.21438, PubMed: 20146604

Prins, N., & Kingdom, F. A. A. (2018). Applying the model-comparison approach to test specific research hypotheses in psychophysical research using the Palamedes toolbox. *Frontiers in Psychology*, *9*, 1250. https://doi.org/10.3389/fpsyg.2018.01250, PubMed: 30083122

Rassi, E., Fuscà, M., Weisz, N., & Demarchi, G. (2019). Detecting pre-stimulus source-level effects on object perception with magnetoencephalography. *Journal of Visualized Experiments*, e60120. https://doi.org/10.3791/60120, PubMed: 31403630

Rassi, E., Wutz, A., Müller-Voggel, N., & Weisz, N. (2019). Prestimulus feedback connectivity biases the content of visual experiences. *Proceedings of the National Academy of Sciences, U.S.A.*, *116*, 16056–16061. https://doi.org/10.1073/pnas.1817317116, PubMed: 31332019

Rubin, E. (1915). *Synsoplevede figurer: studier i psykologisk analyse (Vol. 1)*. Copenhagen: Gyldendal, Nordisk forlag.

Ruhnau, P., Hauswald, A., & Weisz, N. (2014). Investigating ongoing brain oscillations and their influence on conscious perception—Network states and the window to consciousness. *Frontiers in Psychology*, *5*, 1230. https://doi.org/10.3389/fpsyg.2014.01230, PubMed: 25400608

Sadaghiani, S., Hesselmann, G., & Kleinschmidt, A. (2009). Distributed and antagonistic contributions of ongoing activity fluctuations to auditory stimulus detection. *Journal of Neuroscience*, *29*, 13410–13417. https://doi.org/10.1523/JNEUROSCI.2592-09.2009, PubMed: 19846728

Summerfield, C., & Egner, T. (2009). Expectation (and attention) in visual cognition. *Trends in Cognitive Sciences*, *13*, 403–409. https://doi.org/10.1016/j.tics.2009.06.003, PubMed: 19716752

Tong, F., Nakayama, K., Vaughan, J. T., & Kanwisher, N. (1998). Binocular rivalry and visual awareness in human extrastriate

cortex. *Neuron*, *21*, 753–759. https://doi.org/10.1016/S0896-6273(00)80592-9, PubMed: 9808462

van Kerkoerle, T., Self, M. W., Dagnino, B., Gariel-Mathis, M.-A., Poort, J., van der Togt, C., et al. (2014). Alpha and gamma oscillations characterize feedback and feedforward processing in monkey visual cortex. *Proceedings of the National Academy of Sciences, U.S.A.*, *111*, 14332–14341. https://doi.org/10.1073/pnas.1402773111, PubMed: 25205811

Van Veen, B. D., van Drongelen, W., Yuchtman, M., & Suzuki, A. (1997). Localization of brain electrical activity via linearly constrained minimum variance spatial filtering. *IEEE Transactions on Biomedical Engineering*, *44*, 867–880. https://doi.org/10.1109/10.623056, PubMed: 9282479

Walker, P. (1978). Binocular rivalry: Central or peripheral selective processes? *Psychological Bulletin*, *85*, 376–389. https://doi.org/10.1037/0033-2909.85.2.376

Weisz, N., Wühle, A., Monittola, G., Demarchi, G., Frey, J., Popov, T., et al. (2014). Prestimulus oscillatory power and connectivity patterns predispose conscious somatosensory perception. *Proceedings of the National Academy of Sciences, U.S.A.*, *111*, E417–E425. https://doi.org/10.1073/pnas.1317267111, PubMed: 24474792

Willems, R. M., Peelen, M. V., & Hagoort, P. (2010). Cerebral lateralization of face-selective and body-selective visual areas depends on handedness. *Cerebral Cortex*, *20*, 1719–1725. https://doi.org/10.1093/cercor/bhp234, PubMed: 19889713

Wutz, A., Melcher, D., & Samaha, J. (2018). Frequency modulation of neural oscillations according to visual task demands. *Proceedings of the National Academy of Sciences, U.S.A.*, *115*, 1346–1351. https://doi.org/10.1073/pnas.1713318115, PubMed: 29358390

Zazio, A., Ruhnau, P., Weisz, N., & Wutz, A. (2021). Pre-stimulus alpha-band power and phase fluctuations originate from different neural sources and exert distinct impact on stimulus-evoked responses. *European Journal of Neuroscience*, 1–13. https://doi.org/10.1111/ejn.15138, PubMed: 33539589

Zeki, S., & Bartels, A. (1999). Toward a theory of visual consciousness. *Consciousness and Cognition*, *8*, 225–259. https://doi.org/10.1006/ccog.1999.0390, PubMed: 10448004